PMM U.S.S.R., Vol. 46, No. 5, pp. 687-696, 1983.
Printed in Great Britain.

0021-8928/83 $7.50+0.00

UDC 532.546.06

ANALYSIS OF TWO-DIMENSIONAL STEADY-STATE FILTRATION INTO A SOIL LAYER WITH A STRONGLY PERMEABLE FOUNDATION*

V.N. EMIKH

By means of conformal mappings, a hydrodynamic solution of the periodic steady-state nonartesian filtration problem is solved for the case of a system of channels in a homogeneous soil layer subjacent to a highly permeable artesian water horizon, assuming there is drainage and uniform infiltration to the free surface or evaporation from it. A system of equations for the unknown parameters of the mapping is derived, and its unique solvability for definite constraints on the physical parameters of the model established. An algorithm for computing the basic filtration characteristics in the direct formulation and for finding the boundary points at which the current separates into flows at different directions and also for computing the flow rates of each flow is programmed for a computer. In the subsequent analysis, the role of horizontal drainage and other factors is elucidated, and their influence on the shape of the depression curve determined. Limiting flow cases are studied, for example, current without horizontal drainage, current where there is complete ponding surface, and current where there is no ponding (V.V. Vedernikov problem /1/). Certain related problems obtained as a result of continuing the solution for the basic model relative to the parameters of the mapping are considered.

1. Basic model. In Fig.1a may be found a schematic representation of nonartesian steady-state filtration in a homogeneous soil layer T units thick where filtration proceeds from a system of periodically arranged channels into tubular drains lying in the midst of the channels and at the same depth. It is assumed that there is uniform infiltration to the free surface or evaporation from it at a rate ε and at a constant head $h = -H$ at the base of the soil layer which is equal to the head in an subjacent, strongly permeable water horizon. In the current half-period under consideration, the channel is modeled by a linear source GE along which $h = 0$, and the drain by a point outlet B located at a depth β from the surface. The distances between the edges of the neighboring channels and between the neighboring drainage effluents amount to $2l$ and $2L$, respectively. We agree to use the reduced complex coordinate $z = x + iy$ and the reduced complex potential $\omega = \varphi + i\psi$ which are related to reduced physical quantities z_{ph} and ω_{ph} by the relationships ($\varkappa$ is the filtration coefficient)

$$z = z_{ph}/T, \quad \omega = \omega_{ph}/(\varkappa T) \tag{1.1}$$

We introduce the Joukovskii function $\theta = \omega + iz$ /2/ and Numerov function $\Omega = \omega + i\varepsilon z$ /3/. By means of a conformal mapping of the regions θ and Ω (Fig.1b,c) to the half-plane $\operatorname{Im}\zeta \geqslant 0$ (Fig.1d), we find

$$z = i\frac{\Omega - \theta}{1-\varepsilon}, \quad \omega = \frac{\Omega - \varepsilon\theta}{1-\varepsilon} \tag{1.2}$$

$$\Omega = \frac{(1+b)\sqrt{d-g}}{b+r} M \int_{\zeta}^{g} \frac{(r-u)\,du}{(b+u)\sqrt{(d-u)(1-u)(g-u)}} + iQ_* = \tag{1.3}$$

$$M\left[\frac{1-g}{b+g}\Pi\left(\arcsin\sqrt{\frac{g-\zeta}{1-\zeta}}, \frac{1+b}{b+g}, k'\right) + \frac{r-1}{b+r}F\left(\arcsin\sqrt{\frac{g-\zeta}{1-\zeta}}, k'\right)\right] + iQ_*; \quad -b < \zeta \leqslant g$$

*Prikl.Matem.,Mekhan,46,No.5,pp.857-868,1982

$$\theta = i\frac{(1+b)\sqrt{d}}{b-f}M_0\int_0^{\zeta}\frac{(f+u)\,du}{(b+u)\sqrt{(d-u)(1-u)u}} + iQ_s = \tag{1.4}$$

$$M_0\left[\frac{1+b}{b-f}F(\arcsin\sqrt{\zeta},k_0) - \frac{1+b}{b}\Pi\left(\arcsin\sqrt{\zeta},-\frac{1}{b},k_0\right)\right] + iQ_s;\quad 0\leqslant\zeta\leqslant 1$$

$$M = \frac{2Q}{\pi}\sqrt{\frac{(b+g)(b+d)}{(1+b)(d-g)}},\quad k' = \sqrt{1-k^2},\quad k = \sqrt{\frac{1-g}{d-g}} \tag{1.5}$$

$$M_0, k_0 = (M,k)_{g=0}$$

Here Q and $Q_s = Q_c + \varepsilon l$ are the filtration rates of the drainage and the surface water; Q_c, flow rate from the channel within the region under consideration; F and Π, elliptical integrals of the first and second kind in the normal Legendre form.

In the case of the complex speed $w = w_x - iw_y$ we have from (1.2)—(1.4)

$$w = \frac{d\omega}{dz} = -i\frac{d\Omega/d\zeta - \varepsilon\, d\theta/d\zeta}{d\Omega/d\zeta - d\theta/d\zeta} = -i\frac{B-\varepsilon W(\zeta)}{B-W(\zeta)} \tag{1.6}$$

$$W(\zeta) = \frac{f+\zeta}{\zeta-r}\sqrt{\frac{\zeta-g}{\zeta}},\quad B = \frac{b-f}{b+r}\sqrt{\frac{b+g}{b}} = W(-b)$$

Within the framework of the basic model, the following conditions must hold:

$$f\in[0,\ b],\quad r\in[-b,\ g] \tag{1.7}$$

These conditions govern the position of the pressure maximum point F on the segment AB and the point R at which $\overline{w} = i\varepsilon$ on the boundary. As will be explained below, these relations ultimately impose constraints on the physical parameters of the model.

For a given value of Q, the flow rate Q_s and the five parameters of the mapping (b, d, g, f, and r) are to be determined. Once we know the values of L, l, β, T, H, and ε, we may then use the representations (1.2)—(1.4) to arrive after some algebra at a system of equations for these parameters (in terms of (1.1) we have $T = 1$):

$$f_1(b,d,g,r) = K'\left[\frac{r-1}{b+r}M - \frac{2Q}{\pi}Z(\alpha,k')\right] = H-\varepsilon \tag{1.8}$$

$$f_2(b,d,f) = K_0'\left[\frac{1+f}{b-f}M_0 + \frac{2Q}{\pi}Z(\alpha_0,k_0')\right] = 1-H$$

$$(k_0' = \sqrt{1-k^2})$$

$$f_3(b,d,g) = (H-\varepsilon)\frac{K}{K'} - (1-H)\frac{K_0}{K_0'} -$$

$$Q\left[\frac{F(\alpha,k')}{K'} - \frac{F(\alpha_0,k_0')}{K_0'}\right] = (1-\varepsilon)L$$

$$f_4(b,d,g,f) = M_0\left[\frac{1+b}{b-f}F(\arcsin\sqrt{g},k_0) -\right.$$

$$\left.\frac{1+b}{b}\Pi\left(\arcsin\sqrt{g},-\frac{1}{b},k_0\right)\right] = (1-\varepsilon)l$$

$$f_5(b,d,g,f,r) = (1-\varepsilon)y_A + \frac{(1+b)(f+r)}{(b+r)(b-f)}M_0\cdot F(\alpha_0,k_0') -$$

$$\frac{Q}{\pi}\frac{g\sqrt{(1+b)(b+d)}}{b+r}\int_0^{\zeta}\times$$

$$\frac{(r+u)\,du}{[\sqrt{b(g+u)}+\sqrt{(b+g)u}]\sqrt{u(g+u)(1+u)(d+u)}} = (1-\varepsilon)\beta$$

Here Z is the Jacobi zeta function /4/. The ordinate y_A of the point A of the depression curve is determined by the expression

$$y_A = \frac{\operatorname{Re}\Omega(0)}{1-\varepsilon} = \frac{M}{1-\varepsilon}\left[\frac{1-g}{b+g}\Pi\left(\arcsin\sqrt{g},\frac{1+b}{b+g},k'\right) + \frac{r-1}{b+r}F(\arcsin\sqrt{g},k')\right] \tag{1.9}$$

The flow rate Q_s obeys the formula

$$Q_s = (H-\varepsilon)\frac{K}{K'} + Q\left[1-\frac{1}{K'}F\left(\arcsin\sqrt{\frac{b+g}{1+b}},k'\right)\right] + \varepsilon L \tag{1.10}$$

By the first equation of (1.8), the second condition of (1.7) obviously holds whenever $\varepsilon\leqslant H$, $Q>0$; the constraints on ε will henceforth be improved. After several transformations of the second equation of (1.8), we may prove that whenever $Q>0$, the relation $f<b$ also holds. The limiting case $f=0$ is worth noting. Using the integral representations (1.3)

and (1.4), substitution of which in (1.2) leads to the complex-parameter equation of the depression curve, we find that $(dy/dx) \underset{\zeta=0}{=} -\infty$ if $f = 0$; that is, the point A becomes the cusp of the depression curve. By (1.4), we have $\mathrm{Re}\,\theta > 0$, $p < 0$ on the remaining portion of AB, and a further reduction in the pressure p in the drainage zone will lead to leakage of air into it. Such a critical drainage mode had even be noted by V.V. Vedernikov /5/.

Let us study the solvability of the system (1.8). Assuming that the parameter b is still fixed, we consider the third and fourth equations as a subsyatem in the parameters d and g:

$$F_3(d) = f_3[d, g(d)] = (1-\varepsilon)L \qquad (1.11)$$
$$F_4(d, g) = f_4[d, g, f(d)] = (1-\varepsilon)l$$

In this notation, $F_3(d)$ is a composite function of d. The parameter $g(d)$ is determined in this function from the fourth equation of (1.8), while the parameter $f(d)$ in the latter equation is determined from the second equation in (1.8).

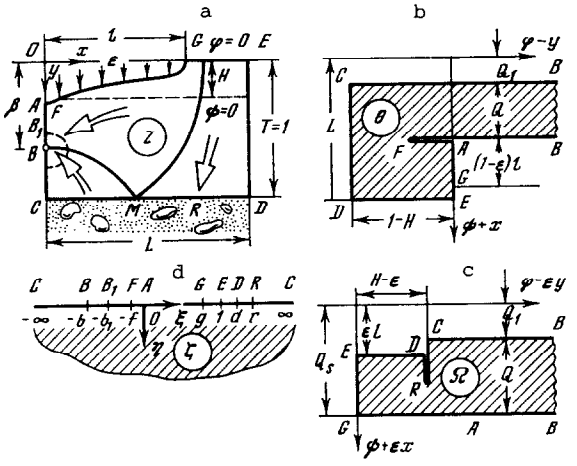

Fig.1

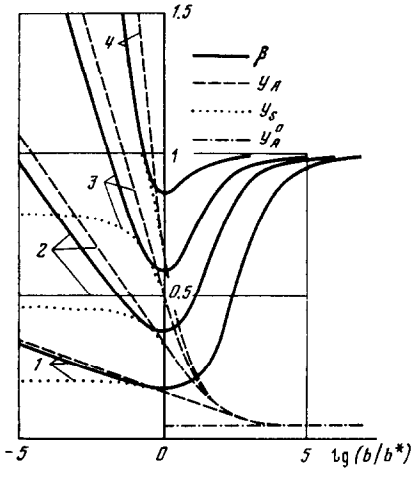

Fig.2

Differentiating the left sides of equations (1.11) with respect to the parameters d and g /4/, we find that, by (1.7) and (1.5) and the first two equations in (1.8),

$$\frac{\partial f_3}{\partial g} = -\frac{\pi M(1+b)(r-g)}{4K'(1-g)(b+r)(b+g)} < 0 \qquad (1.12)$$

$$\frac{\partial f_3}{\partial d} = -\frac{\pi(1+b)}{4(d-1)(b+d)}\left(\frac{M}{K'}\frac{r-d}{b+r} + \frac{M_0}{K_0'}\frac{f+d}{b-f}\right) <$$
$$-\frac{\pi(1+b)}{4(d-1)(b+d)K'}\left(M\frac{g-d}{b+g} + M_0\frac{d}{b}\right) =$$
$$-\frac{Q}{2(d-1)K'}\sqrt{\frac{1+b}{b+d}}\left(\sqrt{\frac{d}{b}} - \sqrt{\frac{d-g}{b+g}}\right) < 0$$

$$\frac{\partial F_4}{\partial g} = \frac{Q}{\pi}\frac{f+g}{(b+g)(b-f)}\sqrt{\frac{b(1+b)(b+d)}{g(1-g)(d-g)}} > 0 \qquad (1.13)$$

$$\frac{\partial F_4}{\partial d} = -\frac{Q}{2\pi}\frac{d+f}{b-f}\sqrt{\frac{b(1+b)}{b+d}}\int_0^g\left(\frac{u}{d-u} + \frac{E_0' - k_0^2K_0'}{k_0'^2K_0'}\right)\times\frac{du}{\sqrt{u(1-u)(d-u)}} < 0$$

As a result, we find that

$$\frac{dF_3(d)}{dd} = \frac{\partial f_3}{\partial d} - \frac{\partial f_3}{\partial g}\left(\frac{\partial F_4}{\partial d}\Big/\frac{\partial F_4}{\partial g}\right) < 0 \qquad (1.14)$$

By (1.13), the function $g(d)$ determined by the second equation of (1.11) increases monotonically, and since $0 \leqslant g < 1$ then $d < d_1$; the value of d_1 is found from the equation $F_4(d_1, 1) = (1-\varepsilon)l$. Since $F_3(1) = \infty$, and $F_3(d_1) = F_4(d_1, 1)$, we conclude that (bearing in mind (1.14)) whenever $L > l$, the first equation of (1.11) has a unique root in the interval $(1, d_1)$.

Thus, for a fixed value of b and under the conditions (1.7), the parameters d, g, f and r are found uniquely from the first four equations of (1.8), while the fifth equation determines β as a function of b. The relation $\beta(b)$ was studied numerically.

In Fig.2 the relation is represented by the solid lines $L = 1.5, l = 1.35, H = 0.05$ and $\varepsilon = 0$ for $Q = 0.05; 0.2; 0.5$ and 2.0 (curves *1–4*, respectively). In the case of fixed flow rate Q, the function $\beta(b)$ attains its minimum $\beta^*(Q)$ at some value $b^* = b^*(Q)$, such that $f = 0$; in this series, it was found that $b^* = 0.00292; 0.04595; 0.2839; 4.479$. Further, we have $f > 0$ if $b > b^*$ and $f < 0$ if $b < b^*$. The interval $(b^*(Q), \infty)$ of values of the parameter b is, consequently, acceptable within this model; segments of the curves on the right of the y-axis correspond to this interval in Fig.2. If β belongs to the interval $(\beta^*(Q), 1)$, this means that the sink may operate with a selected flow rate $2Q$ only if it is at a depth not less than $\beta^*(Q)$. If $\beta = \beta^*$, it will work with a flow rate of $2Q$ in the critical mode ($f = 0$), though this flow rate is not attainable if the sink is located at a higher point. The broken lines, which represent the relation $y_A(b, Q)$ (cf. (1.9), asymptotically approach the line $y = y_A^\circ = y_A|_{Q=0} = 0.04406$ as $b \to \infty$ and $\beta \to 1$; that is, the influence of the sink on the depression curve attenuates without bound as it approaches the lower horizon. The meaning of the dotted lines will be explained in Sect.4.

Passing now to the initial formulation, we conclude, based on the foregoing remarks, that whenever $\beta = \beta^\circ \in (y_A^\circ, 1)$, the choice of Q is bounded by some value of $Q^*(\beta^\circ)$ corresponding to the critical mode; the curve $\beta(b, Q^*)$ comes into contact with the line $\beta = \beta^\circ$ while the curves $\beta(b, Q)$ if $Q < Q^*$ cross it. The monotonic nature of the relation $\beta(b)$ in the interval $(b^*(Q), \infty)$ of acceptable values of b established by the computations is used to find the interval using the fifth equation of the system (1.8). In the process of the numerical solution of this equation for each of the selected values of b, the parameters d, g, f and r are determined from the first four equations of the system.

One possible formulation involves determining the magnitude of the pressure H_d at some point B_1 with coordinate $z = i\beta_1$ (Fig.1a); the equipotential passing through it approximates the actual shape of the sink. As is shown by computations, a monotone increase in H_d accompanies an increase in Q, consequently $H_d \in (H_d^\circ, H_d^*)$ if $Q \in (0, Q^*)$.

Computation of the basic characteristics of the current in this formulation together with a determination of the values of $L, l, H, \varepsilon, \beta, \beta_1$ and H_d was programmed in the Alpha language for the BESM-6 computer. At first we computed both limiting cases which serve to bound the basic model, i.e., $Q = 0$ and $Q = Q^*$. Further, for $H_d \in (H_d^\circ, H_d^*)$, the corresponding value of Q is determined by iterations with interpolation on each iteration. On the first step a linear interpolation is performed using the values of H_d and Q for the above limiting cases as the reference values; then a quadratic interpolation is performed. In all the computation examples, the value of H_d even on the third iteration approaches its specified value with a relative error of 10^{-4}. Thus, for the variant $L = 2.5, l = 2.25, \beta = 0.4, \beta_1 = 0.3875, H = 0.1, H_d = 0.38$, and $\varepsilon = 0$, we find that $Q^{(i)} = 0.1613, 0.1647$, and 0.1649 after first computing the values of $H_d^\circ = 0.0980, Q^* = 0.1819$, and $H_d^* = 0.4160$; correspondingly, $H_d^{(i)} = 0.3731, 0.37966$, and 0.380001 ($i = 1, 2, 3$). N.S. Kolodei participated in the compilation of the program and in the computations.

2. Hydraulic and reclamation analysis of the current. A direct approach in the computations can be used to study the role of each of the characteristic physical parameters of the model. Of particular interest is the analysis of the structure of the current, which may be divided into flows of different directions; in the case of evaporation, for example, there exist seven possible branching alternatives. In concrete examples, the program must anticipate the discovery of a corresponding alternative along with the limiting points of the flow interface and the flow rate of each current.

In Fig.3 may be found the flow pattern for $L = 2.5, l = 2.25, H = 0.1, \beta = 0.4, \beta_1 = 0.3875$, and $H_d = 0.38$. The solid lines and values of the flow rates in the unbroken circles correspond to $\varepsilon = -0.1$, and in the broken circles to $\varepsilon = 0.1$. The depression curves for $Q = 0$ and $Q = Q^*$ are indicated by the markers (∘) and (*), which are appended, in the limiting cases, also to the flow characteristics. Within the region the separating lines of flow are plotted in an approximation.

In the alternative with evaporation, the basic computational mode with values $H_d = 0.38$, $Q = 0.1228$, and $y_A = 0.3401$ is characterized by the dominance of ascending flows near the critical flow at which $H_d = 0.3966$, $Q = 0.1294$, and $y_A = 0.3771$; further, the difference between the depression curves for these modes is captured in Fig.3 only above the sink. The latter absorbs only the underground water and substantially reduces the groundwater level only in its immediate neighborhood; in the process of reclamation, this drainage system is not considered feasible /6/. In the second case, the current is adjusted. Surface water now predominates over underground water in the drainage effluent, and the amount of underground water

that infiltrates is markedly reduced from its level in the preceding alternative. Infiltration is analogously reflected in filtration from the channel; thus when $\varepsilon = -0.1$ and 0.1 we have $Q_c = 0.0933$ and $Q = 0.0301$, respectively.

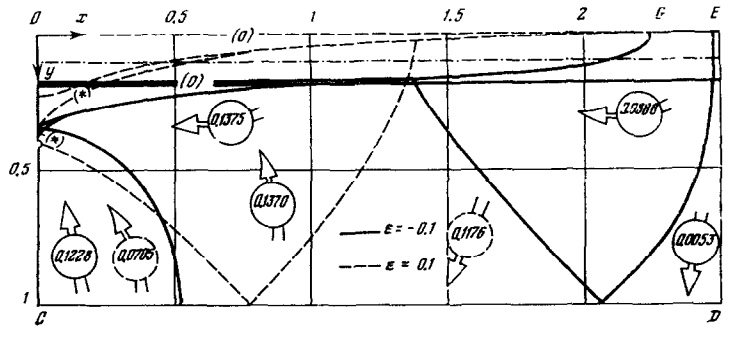

Fig. 3

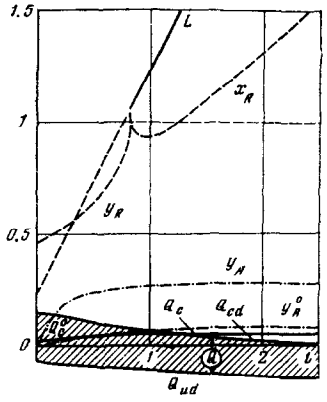

Fig. 4

Such an attenuation trend for the role of one factor that affects current in opposite ways, once its opposing factor is activated (infiltration and replenishment from a pressure stratum and filtration of river water and precisely such factors) are of the nature of laws in these processes. It is also seen in Fig. 4, which is constructed for the case $H = 0.1$, $\beta = 0.4$, $\beta_1 = 0.3875$, $H_d = 0.38$, and $\varepsilon = 0$ with $L - l = 0.25$, i.e., for a fixed width of the channel. As l and L increase, while the seepage rate of the sink Q decreases overall, its component Q_{cd} decreases due to the channel, but in addition the proportion of the underground water Q_{ud} increases. A second result of this trend is seen in the increase in outflow from the channel in the lower horizon which competes with the sink, but in proportion to its distance from the horizon; the overall seepage rate from the channel Q_c decreases in this case. The fact that the curves Q_c and Q_c^0 approach each other indicates the interaction between the channel and sink attenuates with increasing l. The broken lines indicate the dynamics of the point R which, in the case $\varepsilon = 0$, is a limiting point at the separation between the flows. As l increases, it turns, together with the segment ED, into the base (when $l = 0.807$) and then moves along the base, completing a return motion immediately before the transition.

Infiltration plays a major role in the formation of the current. As we noted earlier, an increase in infiltration is compensated by drainage, the function of which may be also carried out by the lowest horizon; at the same time, inflow of river and underground water into the soil layer reduces, and the free surface rises. According to computations, as ε increases the point B, which is the section top point of the region Ω (Fig. 1c), moves along the boundary towards the point G, merging with it at some definite value $\varepsilon = \varepsilon^*$.

To study the flow transformations occurring here, let us return to the depression curve. Bearing in mind its complex parameter equation (1.2), and substituting in the latter the integral representations (1.3) and (1.4) for the functions Ω and θ, we find that

$$\frac{dy}{dx} = \frac{dy/d\zeta}{dx/d\zeta} = -\frac{b-f}{b+r}\sqrt{\frac{b+g}{b}\,\frac{r-\zeta}{f+\zeta}}\sqrt{\frac{\zeta}{g-\zeta}}; \quad 0 \leqslant \zeta \leqslant g \tag{2.1}$$

$$\frac{d^2y}{dx^2} = -\frac{\pi(1-\varepsilon)(b-f)^2\sqrt{b+g}}{2Qb(b+r)\sqrt{(1+b)(b+d)}}\,\frac{P(\zeta)(b+\zeta)\sqrt{(1-\zeta)(d-\zeta)}}{(f+\zeta)^3\sqrt{(g-\zeta)^3}} \tag{2.2}$$

$$P(\zeta) = (2r+2f-g)\zeta^2 - g(3f+r)\zeta + fgr =$$
$$(2r+2f-g)(\zeta - r_1)(\zeta - r_2)$$

$$r_{1,2} = \frac{g(3f+r) \pm r\sqrt{g(1+f/r)(g-8f-9fg/r)}}{2(2r+2f-g)}$$

By (2.1), when $\varepsilon = \varepsilon^*$ and $r = g$, we have $dy/dx = 0$ for $\zeta = g$. Such smoothing out of the depression curve at point G indicates the onset of underflooding, which develops with a subsequent increase in ε, but now within the framework of a different hydrodynamic scheme, where $r < g$ (cf. Sect. 4). The quantity ε^* is the maximally acceptable value of ε in the basic model and is related to the other physical parameters and is computed in each particular alternative.

Thus in the case $L = 1.5$, $l = 1.35$, $H = 0.05$, $\beta = 0.4$, $\beta_1 = 0.3875$, and $H_d = 0.38$, we find that $\varepsilon^* = 0.0979$. Note that without drainage a complete underflooding along with emergence of the entire depression curve AG on the surface occurs at $\varepsilon = H$ /7/, and consequently, at $Q = 0$, $\varepsilon^* = 0.05$ in this alternative; drainage seems to create a reserve for an increase in infiltration.

According to (2.2), the roots r_1 and r_2 of the trinomial $P(\zeta)$ are real whenever the following inequality is fulfilled:

$$g - 8f + 9fg/r > 0 \tag{2.3}$$

If, in addition, the constraints (1.7) are satisfied, then, as can be verified, $r_{1,2} \in (0, g)$; the curve AG has two inflection points, and, along with the general decrease in the ground water, there occurs an additional local depression directly over the sink.

Based on the first two equations of the system (1.8), we may prove that $\lim r = -b - 0$, $\lim(-f) = -b + 0$ as $Q \to 0$ (cf. Fig.1d), consequently, $g - 8f + 9fg/r = -8(b + g) < 0$ when $Q = 0$, i.e., the curve AG is concave throughout its length. Thus a local depression is completely attributable to artificial drainage and, according to (2.3), clearly arises when drainage is increased, which, as was explained in Sect.2, accompanies a decrease in the parameter f. From this standpoint, it is natural to consider a local depression as a state that precedes the breakdown of the dynamic equilibrium of the depression curve when $Q \geq Q^*$.

By (2.3), the appearance of inflection points on AG is predetermined once infiltration increases, since $D \approx g + f > 0$ if $\varepsilon \approx \varepsilon^*$, $r \approx g$. Also, here artificial drainage becomes an indispensable condition for the inequality (2.3); however, in this situation, which, as noted above, precedes underflooding, it is more proper to speak not of a local depression, but rather of a local rise of the ground water level in a neighborhood of the channel.

In the above examples, we have found a comparatively low efficiency of the horizontal drainage where there is a further powerful drainage factor, such as a highly permeable subjacent stratum.

This conclusion is also clear if we consider Table 1, in which the values of the inflow to the sink from below Q_{ud}, and the surface Q_{sd}, and the outflow Q_{su} of surface water to the subjacent horizon are presented, as computed for several values of H and for $Q = Q^*$ in the case $L = 2.5540$, $l = 2.3008$, $\beta = 0.3822$, and $\varepsilon = 0$, i.e., within the limits of the capacity of the sink. At low H, these capacities seem at first glance to be significant, particularly if it is borne in mind that for a system with a confining stratum /8/ at these values of the parameters L, l, β, and ε, we have $Q^* = 0.0759$, though deep-lying water is basically drained, while the drainage system, as already noted, does not meet the purpose designated for it /6/. As H incrases, it in fact becomes inoperable. However, in accordance with the above law, at some stage of attenuation of the effluent, entry of surface water into the sink is activated as the seepage flow rate Q_s of the surface water increases in general, thereby partially compensating the shortage from the subjacent stratum.

Table 1

H	0	0.1	0.2	0.3
$Q^* \times 10^4$	2509	1650	912	324
$Q^*_{ud} \times 10^4$	2453	1389	692	204
$Q^*_{sd} \times 10^4$	56	261	220	119
$Q^*_{su} \times 10^4$	0	391	948	1479

3. Limiting cases. We now wish to discuss several flow systems that are limiting with respect to the above basic model.

Filtration without artificial drainage. In a study of artificial drainage /7/, the decrease in the seepage flow rate from a channel together with an increase in infiltration or effluent was explained analytically. Attenuation of the effluent, by contrast, leads to a significant (roughly exponential halfway between the channels) decrease in the rise in the ground water from the channel and to a drop in the length of the zone within which this rise occurs; this confirms the well-known interpretation of vertical drainage as an effective means of water drawdown. At low effluent values, such flow is close to that considered previously by S.N. Numerov /9/ for an isolated channel system.

Complete ponding. In this case the expression for ω is obtained from (1.3) with $g = 0$. Further we have

$$z = \frac{L}{2K}\int_0^{\zeta}\frac{du}{\sqrt{u(1-u)(1-k^2u)}} = \frac{L}{K}F(\arcsin\sqrt{\zeta}, k) \tag{3.1}$$

The modulus k of the elliptical integral is determined from the equation

$$K/K' = L \tag{3.2}$$

Expression (1.10) is reduced, by means of (3.1) and (3.2), to the form

$$Q_s = HL + Q(1-\beta) \tag{3.3}$$

At low values of k, the approximation relations

$$k' \approx 4e^{-\pi L/2},\quad K' \approx \frac{\pi}{2},\quad K \approx \ln\frac{4}{k'} \tag{3.4}$$

are satisfied; based on these relations we find that, for example, with $R \in CD$,

$$Q \approx (H_d - \beta_1 H)\left(\frac{2}{\pi}\operatorname{arth}\sqrt{\frac{b_1}{b}}\right)^{-1};\quad b \approx \operatorname{tg}^2\frac{\pi\beta}{2};\quad b_1 \approx \operatorname{tg}^2\frac{\pi\beta_1}{2} \tag{3.5}$$

$$Q_{ud} \approx \frac{2Q}{\pi}\operatorname{arctg}\sqrt{\frac{b}{r}} - Hx_R;\quad x_R \approx \frac{2}{\pi}\operatorname{arcth}\sqrt{r};\quad r \approx \frac{Q\sqrt{b}+bH}{Q\sqrt{b}-H}$$

The relative error of these formulas $\delta = O(k')$, therefore they may be used beginning with values of $L \approx 3-4$.

In this case, we have for the seepage rate

$$\bar{w} \approx i\left(H + Q\sqrt{b}\,\frac{1-\zeta}{b+\zeta}\right) \tag{3.6}$$

In accordance with (3.6) and (3.1), we may write

$$1-\zeta = O(k'),\quad \bar{w} = iH + O(k'),\quad L/2 \leqslant x \leqslant L \tag{3.7}$$

for the points of the right half of the filtration region /10/.

Thus flow here is close to the one-dimensional descending case, and the influence of the sink is manifest only in some neighborhood of the sink. Such localization is reflected in Fig.5, which is constructed using computations for $L = 2.5, H = 0.1, \beta = 0.4, \beta_1 = 0.3875$, and $H_d = 0.38$. In the case under study, the role of horizontal drainage in the diversion of surface water becomes more important than in partial ponding, though its effectiveness here is determined largely by the pressure in the subjacent stratum; this is clear from the first formula in (3.5).

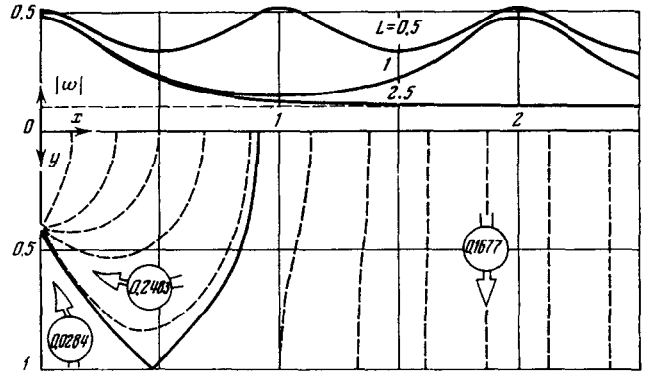

Fig.5

This limiting case may be interpreted also as planned filtration to a completed well sunk in a band-shaped stratum along a line parallel to its constant pressure boundaries.

Drainage of unflooded soil layer. In this case Vedernikov constructed a solution using conformal mappings /1/. In /11/, the problem was solved in a different way using the Fourier method and numerical computations. We will proceed here from the Vedernikov solution, which may be obtained from (1.2)—(1.5) by a transition to the limit as $g, r \to 1$. In the notation of the article, the equation of the depression curve is written in the form

$$z = \frac{M_0(1+b)}{(1-\varepsilon)(b-f)}\left[F(\arcsin\sqrt{\zeta}, k_0) - \frac{b-f}{b}\Pi\left(\arcsin\sqrt{\zeta}, -\frac{1}{b}, k_0\right)\right] + i\frac{1}{1-\varepsilon}\left(\frac{2Q}{\pi}\operatorname{arth}\sqrt{\frac{d-\zeta}{b+d}} + H - \varepsilon\right);\quad 0 \leqslant \zeta \leqslant 1 \tag{3.8}$$

The parameters b, d and f are found from the second, third, and fifth equations of the system (1.8); in the last two equations, it is first necessary to perform this transition to the limit. In Table 2 may be found values of Q, y_A, and y_E computed for $L = 1.5$, $H = 0.05$, $\beta = 0.4$, $\beta_1 = 0.3875$, and $H_d = 0.38$ for several values of the parameter ε. An increase in ε induces drainage and a rise in the depression curve, whose highest point E at $\varepsilon = 0.09346$ reaches the surface of the soil, while when $\varepsilon = 0.1$ it is already above it. At values of ε at which part of the surface is flooded, the flow must be considered within the framework of the basic model

which, consequently, is a natural extension of the Vedernikov problem.

Table 2

ε	−0.5	−0.3	−0.1	0.1
$Q\times10^4$	201	1469	3060	4797
$y_A\times10^4$	3823	3737	3182	1891
$y_E\times10^4$	3671	2743	1545	−61

4. Related systems. Let us discuss certain systems that may be described by (1.2)–(1.5) beyond the limits established by relations (1.7).

1) From an analysis of the second equation of (1.8), we find that $Q<0$ if $f<b$, which corresponds to flow from a forced drain.

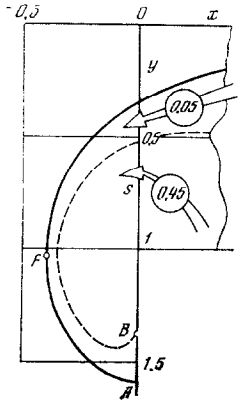

Fig.6

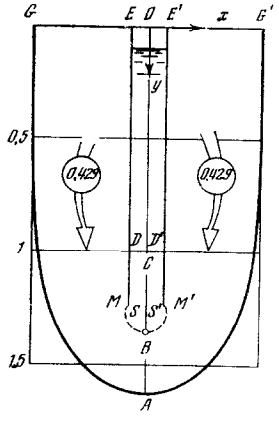

Fig.7

2) As remarked in Sect.2, the inequality $r<g$ is true when $\varepsilon>\varepsilon^*$. For this combination of the physical parameters with a value $\varepsilon^*=0.0979$, the computations were also performed for $\varepsilon=0.15$ and $\varepsilon=0.2$; we found $r=0.9534$, $g=0.9917$, $x_R=1.1167$, $y_R=-0.0204$, and $r=0.9089$, $g=0.9876$, $x_R=1.0100$, and $y_R=-0.0486$. The point R is now the vertex of the hillock of ground water formed in a neighborhood of the point G (it is understood that there is soil everywhere there is a flow of water). If $\varepsilon=0.15$, the segment GE operates partially as a slotted drain up to the point with abstissa 1.3990, and when $\varepsilon=0.1$, operates entirely as such a drain. Its vertex with x-value 1.3490 and 1.3463, respectively, is close to the point at which the depression curve reaches the sink ($x_G=l=1.35$). The previously noted features of the flow are also clear from the computational alternatives discussed here; an increase in Q from 0.2578 to 0.2755 accompanies an increase in ε from 0.15 to 0.2, though in this case we have $Q_{ud}=0.0811$ and 0.0647, i.e., replenishment of the sink from below attenuates and, as already noted, filtration into the soil layer from the segment GE halts.

3) A markedly different hydrodynamic meaning is acquired by the system that appears as a result of the continuation of the initial solution into the valuation domain $f<0$; in Fig. 2 it is to the left of the y-axis. Flow whose near-sink fragment is represented in Fig.6 corresponds to the same combination of initial parameters as the curves in series 3 of Fig.2, and to the value $b=b^*\cdot10^{-3}$. Here $f=-0.00855$; the point $F(-0.3870;\ 1.0216)$ is the leftmost point of the depression curve. The flow pattern is similar to that described in /12/ for the case of an isolated sink in a stratum of unbounded thickness. Thus the ground water from the channel and the underlying horizon overflows at a ratio 1:9 from the boundary point of separation of these flows $M(1.5;\ 0.6031)$ across a vertical screen with vertex at the point $S(0;\ 0.7741)$ and captures the drainage effluent from $B(0;\ 1.3596)$ located on the screen surface on the outside of the feeding sources. The dotted line in Fig.2 represents the relation $y_S(b)$ with $b<b^*$; their point of tangency with the solid curves $\beta(b)$ corresponds to the point at which the discharge of B reaches the vertex of the screen followed by a transition to its outer surface.

For each of the computed values of Q, the discharge B and the point A move down along the screen surface to infinity as $b\to0$. Thus with $Q=0.05;\ 0.2$, and 0.5, the curves $y_S(b)$ approach the asymptotes, i.e., the position of S is stabilized. But if $Q=2.0$, it drops to the base of the soil layer once $b\approx b^*\cdot10^{-0.8}$; with a further decrease in the parameter b along the continuation of the roof of the highly permeable horizon, a slot appears that is connected with the latter and that delivers a flow at the same pressure. To prevent bivalent behavior in the flow region, the system described, like analogous ones from /12/, may be interpreted physically solely within the framework of unilateral inflow towards sink.

In the case of the variant depicted in Fig.7 and computed for $H = 0.1$, $\varepsilon = 0$, $Q = 0,8$, $b = 1$, $g = 0.9999$, $d = 10^5$, and $T = 1$, we find that $L = -0.0744$, $l = -0.5016$, and $\beta = 1.3550$. Since the entire filtration region is found in the half-plane $x \leqslant 0$, we may return to the bilateral inflow system, in which case we have the following pattern: drainage flow $B(0; 1.3550)$ below a trench whose pre-image is equal to the underlying horizon with impermeable walls ES and $E'S'$ buried at the level $y = 1.2495$ and a permeable floor DD' (in the initial model, the base of the soil layer). In addition to the flow from the trench, water also drains from the surface, which is flooded on both sides up to the point $G(-0.5016; 0)$ and $G'(0.5016; 0)$, and the flow rates are 0.742 and 0.858, respectively. At the flow boundary, we encounter flows on the wall surfaces external to the drain and at the points M and M' with ordinate 1.2477. Higher up, at $y = 1.2448$, points F and F' are found at which $|w| = w_y = 1$; in this case, they are points of minimum pressure along the segments ESD and $E'S'D'$. As in the preceding system, current here is realized where there is a definite mode for the creation of a vacuum along the segment AB. Once this vacuum is strengthened, this will lead to a gap in the drain below the outside air, and when the vacuum becomes attenuated, part of the ground water is no longer captured by the drain and escapes downward.

Note that this somewhat simplified, though nevertheless more natural modification of the last system (without a trench with walls) leads to the capture problem for horizontal vacuum sinks in which the sinks serve to trap lower-lying ground water layer which may subsequently be returned to the irrigation network.

Characteristic features of the current in the basic and related systems may be explained analytically. Based on (1.6), we have

$$\frac{dw}{d\zeta} = -i\,\frac{B(1-\varepsilon)W'(\zeta)}{[B-W(\zeta)]^2}; \quad W'(\zeta) = -\frac{P(\zeta)}{2(r-\zeta)\sqrt{\zeta^3(\zeta-g)}} \tag{4.1}$$

The quadratic trinomial $P(\zeta)$ determined in accordance with (2.2) has real roots r_1 and r_2 when condition (2.3) holds. As noted in Sect.3, under the constraints (1.7), i.e., within the framework fo the basic model, $r_{1,2} \in (0, g)$, and, consequently, $du/d\zeta \neq 0$ along the entire fixed boundary. In related systems, the situation is different. Based on (2.2), we may prove that, in the case of r_1, the transition of R_1 to the segment GE corresponds to a transition of R to the depression curve AG; on GE, R_1 becomes the maximum point of w_y. At some point of GE (the terminus of the drainage slit), the abscissa $x(\zeta)$ attains a minimum, and the flow rate is infinite; two variants of such flow are described above. Similarly, the points F and R_2 in the limiting case $f = 0$ merge into the point A, and as the parameter f successively decreases, varies its relative position along the boundary, as well as from the standpoint of physics; in this case, the minimum point of the ordinate $y(\zeta)$, or vertex of the screen, appears on the segment AB. According to the foregoing, for a definite combination of the parameters of the mapping, such extrema may also appear on the boundary segments CD and DE. In each particular variant, computations must reflect the values of the coordinates of all the characteristic boundary points and, thus, the basic details of the flow pattern are explained.

In /13, 14/, functional relations for certain filtration systems were used to derive general-type relations between the complex potential and the complex coordinate. A semi-inverse approach allows for the possibility of approximating the form of the individual boundary segments (shape of channel profile, slope of earthen dam) by a given form by varying the constant coefficients in the solution. Subsequently, it was explained /15/ that for certain values of the coefficients these segments may turn out to cross themselves. That is, bivalent behavior is seen in the flow region under its initial physical interpretation. In the case of the multi-parametric problem described above, an analogous disturbance of univalance accompanied by departure from the scope of the basic filtration system whenever $f < 0$.

REFERENCES

1. VEDERNIKOV V.V., Theory of drainage, Dokl. Akad. Nauk SSSR, Vol.59, No.6, 1948.
2. POLUBARINOVA-Kochina P.Ia., Theory of Ground Water Motion, Moscow, NAUKA, 1977.
3. NUMEROV S.N., A method of solving filtration problems in the presence of infiltration or evaporation of liquid from the free surface, Izv. Vses. N.-I. In-ta Gidrotekhn., Vol.38, 1948.
4. BYRD P.F. and FRIEDMANN M.D., Handbook of Elliptic Integrals for Engineers and Scientists, Berlin—Heidelberg—New York, Springer-Verlag, 1971.
5. VEDERNIKOV V.V., Filtration Theory and its Application to Irrigation and Drainage, Moscow — Leningrad, Gosstroiizdat, 1939.

6. AVER'IANOV S.F., Computation of drying action of horizontal drainage under pressurized feeding conditions, Nauchn. Zap. Mosk. In-ta Inzh. Vodn. Kh-va, Vol.22,1960.
7. EMIKH V.N., Ground water conditions in an irrigated soil layer with subjacent highly permeable pressure horizon, Izv. Akad. Nauk SSSR, MZhG, No.2, 1979.
8. EMIKH V.N., Comparison of approximate and exact models of filtration in drainage cleaning of soil with a water-confining stratum, Izv. Akad. Nauk SSSR, MZhG, No.3, 1982.
9. NUMEROV S.N., Filtration from channels of diversion hydroelectric power stations and irrigation systems. Izv. Vses. N.-I. In-ta Gidrotekhn., Vol.34, 1947.
10. BEJTMAN H. and ERDELYI A., Higher Transcendental Functions, Vols.1 and 2. McGraw-Hill, New York, 1953.
11. NUMEROV S.N. and PANASENKO L.A., Problem of filtration of ground water in the presence of systematic drainage, In: Prikl. Matem. No.1 (135), Leningrad, LISI, 1977.
12. EMIKH V.N., On some hydrodynamic models of drainage PMM, Vol.43, No.6, 1979.
13. RIZENKAMPF B.K., Hydraulics of Ground Water. Part 3. Uch. Zap. Sarat. Un-ta, Vol.15, No. 5, 1940.
14. GERSEVANOV N.M., Application of functional analysis for the solution of problems on filtration of ground water, Izv. Akad, Nauk SSSR, OTN, No.7, 1943.
15. TSITSKISHVILI A.R., On the iteration method of N.M. Gersevanov. PMM, Vol.21, No.2, 1957.

Translated by R.H.S.